Deformed charmed hypernuclei

Yi-Xiu Liu (刘益秀),[1] C. F. Chen (陈超锋),[2,*] Q. B. Chen (陈启博),[1] Huai-Tong Xue (薛怀通),[1] H.-J. Schulze,[3] and Xian-Rong Zhou (周先荣)[1,†]

[1]*Department of Physics, East China Normal University, Shanghai 200241, China*

[2]*School of Physics Science and Engineering, Tongji University, Shanghai 200092, China*

[3]*Dipartimento di Fisica, INFN Sezione di Catania, Universitá di Catania, Via Santa Sofia 64, 95123 Catania, Italy*

(Received 3 October 2023; accepted 27 November 2023; published 20 December 2023)

Charmed Λ_c^+ hypernuclei are investigated in the framework of the deformed Skyrme-Hartree-Fock approach. Their ground-state bulk properties, single-particle energy levels, potential energy curves, as well as the existence limit of charmed hypernuclei are studied with particular regard to the effects of deformation. Λ_c^+ $1p$ states are found to be strongly bound, in particular in deformed nuclei.

DOI: 10.1103/PhysRevC.108.064312

I. INTRODUCTION

Charmed hypernuclei may be the only source of information for studying interactions of charmed baryons with nucleons at low energy and related symmetries, which cannot be obtained by other methods due to the short lifetime of charmed particles.

Bound charmed hypernuclei were first discussed in 1977 by Dover and Kahana within SU(4) symmetry [1]. Later, a candidate event with a He, Be, or C core and an assumed Λ_c separation energy between 0 and 10 MeV was found [2], which motivated further theoretical work [3–8]. However, the experimental results have not been on solid ground. Hopefully new experimental programs, such as the GSI-FAIR and JPARC facilities, will provide new experimental data for a better understanding of the properties of hypernuclei [9].

Since Λ_c is a positively charged particle, the Coulomb repulsion with the protons influences the stability of its hypernuclei. In recent decades, the possible existence of charmed hypernuclei was investigated by various theoretical approaches. The first studies within SU(4) one-boson-exchange models assumed or motivated a $\Lambda_c N$ interaction strength similar or slightly weaker than for the strange hyperon, ΛN, and pointed out the possible existence of many Λ_c hypernuclei [6,10–12]. Within the relativistic mean-field (RMF) model, it was found that the spin-orbit (s.o.) splittings for Λ_c hypernuclei are very small and the positive charge of Λ_c plays an important role [13]. Lattice quantum chromodynamics (QCD) calculations (with an unphysical very large pion mass $m_\pi = 410$ MeV) found that the $\Lambda_c N$ interaction is attractive with a similar strength in the $^1S_0$ and $^3S_1$ channels at low energies and predicted that Λ_c hypernuclei can be formed for atomic numbers $A \lesssim 50$ [14]. The same interaction strength was assumed in a quark-mean-field model [15] with compatible results regarding the stability of hypernuclei. This was debated in a perturbative many-body approach [16,17], who pointed out that extrapolation to the physical pion mass yields hypernuclei over the full range of A. Recently, the ground state properties of charmed nuclei were investigated in the Skyrme-Hartree-Fock (SHF) approach [18], which also found Λ_c hypernuclei over the full range of A with a maximum binding around $A \approx 40$, due to the Coulomb repulsion effect.

In general, due to the absence of quantitative experimental data, those different theoretical investigations used different (types of) more or less phenomenological $\Lambda_c N$ interactions, which is the main reason for their varying predictions. We refer to the review in Ref. [19]. For an overview and comparison, we list in Table I the results obtained by different works for the Λ_c mean field in nuclear matter of normal density, U_{Λ_c}. One may conclude that there is a general consensus (or self-imposed restriction) on a reduction of about 20% relative to the binding of the strange Λ in nuclear matter, $U_\Lambda \approx 30$ MeV.

All calculations mentioned above were performed for spherical nuclei. However, it is well known that the ground states of many p- and d-shell nuclei are deformed [20]. For example, ^{8}Be and ^{12}C have large quadrupole moments [21]. Therefore, the purpose of this paper is to extend the calculation of closed-shell spherical hypernuclei to more complex open-shell nuclei and investigate the impact of the $\Lambda_c N$ interaction strength on the hypernuclei [22,23]. The calculations will be carried out in the framework of the deformed SHF (DSHF) model [24–27], which has already been widely applied for the study of various kinds of strangeness nuclei, such as Λ [28–31], Ξ^- [32,33], and K^- [34,35] nuclei. We will discuss the effects of Λ_c on the light hypernuclei and the possible properties of ${}^{9}_{\Lambda_c}$B and ${}^{13}_{\Lambda_c}$N. Here, the notation for the Λ_c hypernuclei follows the chemical convention, where the element name refers to the total charge of the nucleus (including protons and Λ_c^+ charges), as well as the mass number counting nucleons and hyperons. Finally, the range of deformed charmed hypernuclei with varying $\Lambda_c N$ interaction strengths will be estimated.

The paper is organized as follows. In Sec. II, we briefly review the DSHF approach for charmed hypernuclei. In Sec. III,

*cfchen@tongji.edu.cn

†xrzhou@phy.ecnu.edu.cn

TABLE I. Theoretical predictions for the Λ_c potential depth $-U_{\Lambda_c}$ in nuclear matter. No Coulomb interaction is included. ≡ indicates 'ad hoc' values.

Year	Method	Ref.	$-U_{\Lambda_c}$[MeV] or U_{Λ_c}/U_Λ
1978	SU(4) One-boson exchange	[10]	≈ 28
1981	SU(4) One-boson exchange	[11]	≈ 22
1985	SU(4) One-boson exchange	[12]	≈ 24.6
1986	SU(4) One-boson exchange	[6]	$\approx 0.8U_\Lambda$
2004	Relativistic mean field	[13]	$\equiv 30$
2017	Parity-projected QCD sum rules	[36]	≈ 23
2018	Lattice QCD ($m_\pi = 410$ MeV)	[14]	$\lesssim 20$
2019	Heavy quark eff. potential	[37]	$\approx 24 - 28$
2020	Chiral pert. + lattice QCD	[17]	≈ 19
2021	Skyrme-Hartree-Fock	[18]	$\equiv 0.8U_\Lambda$

the properties of deformed charmed hypernuclei are analyzed. Conclusion and prospects are given in Sec. IV.

II. FORMALISM

The SHF mean-field method is a powerful theoretical density-functional formalism, which can be applied comprehensively from light to heavy nuclei [25–27]. Our approach is the axial-symmetric SHF model, which is combined with a density-dependent Skyrme force for the $\Lambda_c N$ interaction. In this self-consistent model, the total energy of a hypernucleus is calculated as [24,38–41]

$$E = \int d^3\boldsymbol{r}\, \varepsilon(\boldsymbol{r}), \quad \varepsilon = \varepsilon_{NN} + \varepsilon_{\Lambda_c N} + \varepsilon_C, \tag{1}$$

where ε_{NN} is the energy density of the nucleon-nucleon interaction, $\varepsilon_{\Lambda_c N}$ is the contribution due to the $\Lambda_c N$ interaction, and ε_C is the energy density of the Coulomb interaction involving protons and Λ_c^+ hyperon. These energy-density functionals depend on the one-body densities ρ_q, kinetic densities τ_q, and s.o. currents $\boldsymbol{J}_q$,

$$[\rho_q,\ \tau_q,\ \boldsymbol{J}_q] = \sum_{i=1}^{N_q} n_q^i \left[|\phi_q^i|^2,\ |\nabla\phi_q^i|^2,\ \phi_q^{i*}(\nabla\phi_q^i \times \boldsymbol{\sigma})/i\right], \tag{2}$$

where ϕ_q^i $(i = 1, N_q)$ are the self-consistently calculated single-particle (s.p.) wave functions of the N_q occupied states for the different particles $q = n, p, \Lambda_c^+$ in a hypernucleus. The occupation probabilities n_q^k are calculated by taking into account pairing within a Bardeen–Cooper–Schrieffer (BCS) approximation for nucleons only. The pairing interaction between nucleons is taken as a density-dependent δ force [42,43],

$$V_q(\boldsymbol{r}_1, \boldsymbol{r}_2) = V_q' \left[1 - \frac{\rho_N((\boldsymbol{r}_1 + \boldsymbol{r}_2)/2)}{0.16\ \text{fm}^{-3}}\right] \delta(\boldsymbol{r}_1 - \boldsymbol{r}_2), \tag{3}$$

where $\rho_N = \rho_p + \rho_n$ is the nucleon density, and pairing strengths $V_p' = V_n' = -410\,\text{MeV fm}^3$ are used for light nuclei [44], while $V_p' = -1146\,\text{MeV fm}^3$, $V_n' = -999\,\text{MeV fm}^3$ for medium-mass and heavy nuclei [20]. A smooth energy cutoff is employed in the BCS calculations [45]. In the case of an odd nucleon number, one has to block particle orbits near the Fermi energy to pick out the largest binding of (hyper)nuclei [46].

The minimization of the total energy in Eq. (1) implies the SHF Schrödinger equation for each s.p. state (q, i),

$$\left[-\nabla \cdot \frac{1}{2m_q^*(\boldsymbol{r})}\nabla + V_q(\boldsymbol{r}) - i\boldsymbol{W}_q(\boldsymbol{r}) \cdot (\nabla \times \boldsymbol{\sigma})\right]\phi_q^i(\boldsymbol{r}) = e_q^i \phi_q^i(\boldsymbol{r}), \tag{4}$$

where the mean fields of nucleons and hyperons (including the Coulomb interaction) are written as

$$V_q = V_q^{\text{SHF}} + V_q^{(\Lambda_c)}, \quad V_q^{(\Lambda_c)} = \frac{\partial \varepsilon_{\Lambda_c N}}{\partial \rho_q}, \quad (q = n, p), \tag{5}$$

$$V_{\Lambda_c} = \frac{\partial \varepsilon_{\Lambda_c N}}{\partial \rho_{\Lambda_c}} + q_{\Lambda_c} V_C, \tag{6}$$

where V_q^{SHF} is the Skyrme mean field of the nucleon without hyperon (but including the modified Coulomb field) [24,38], $V_q^{(\Lambda_c)}$ is its change due to the addition of the Λ_c, and V_{Λ_c} is the Λ_c mean field. The nucleonic s.o. mean field is represented by $\boldsymbol{W}_{n,p}$ and is provided by the NN Skyrme force used here, whereas we assume $\boldsymbol{W}_{\Lambda_c} = 0$ in this work. For the nucleonic energy-density functional ε_{NN} we employ the SLy4 parametrization [25–27,47], while the functional for the hyperonic part is given by Refs. [39–41,48]

$$\begin{aligned}\varepsilon_{\Lambda_c N} = {} & \frac{\tau_{\Lambda_c}}{2m_{\Lambda_c}} + a_0\rho_{\Lambda_c}\rho_N + a_3\rho_{\Lambda_c}\rho_N^2 + a_1(\rho_{\Lambda_c}\tau_N + \rho_N\tau_{\Lambda_c}) \\ & - a_2(\rho_{\Lambda_c}\Delta\rho_N + \rho_N\Delta\rho_{\Lambda_c})/2 \\ & - a_4(\rho_{\Lambda_c}\nabla\cdot\boldsymbol{J}_N + \rho_N\nabla\cdot\boldsymbol{J}_{\Lambda_c}),\end{aligned} \tag{7}$$

which provides the hyperonic SHF mean fields

$$V_{\Lambda_c} = a_0\rho_N + a_3\rho_N^2 + a_1\tau_N - a_2\Delta\rho_N - a_4\nabla\cdot\boldsymbol{J}_N + q_{\Lambda_c}V_C, \tag{8}$$

$$V_N^{(\Lambda_c)} = a_0\rho_{\Lambda_c} + 2a_3\rho_N\rho_{\Lambda_c} + a_1\tau_{\Lambda_c} - a_2\Delta\rho_{\Lambda_c} - a_4\nabla\cdot\boldsymbol{J}_{\Lambda_c}, \tag{9}$$

and a Λ_c effective mass

$$\frac{1}{2m_{\Lambda_c}^*} = \frac{1}{2m_{\Lambda_c}} + a_1\rho_N, \tag{10}$$

where $m_{\Lambda_c} = 2286.5$ MeV [49], more than twice the mass of the strange Λ baryon, $m_\Lambda = 1115.7$ MeV.

The relation to the standard $\Lambda_c N$ Skyrme parameters $t_{0,1,2,3}^{\Lambda_c N}$ is [40]

$$a_0 = t_0, \quad a_1 = \frac{t_1 + t_2}{4}, \quad a_2 = \frac{3t_1 - t_2}{8}, \quad a_3 = \frac{3t_3}{8}. \tag{11}$$

An approximate center-of-mass correction is applied as usual by replacing the bare masses [24–27,38]

$$\frac{1}{m_q} \to \frac{1}{m_q} - \frac{1}{M}, \tag{12}$$

where $M = (N_n + N_p)m_N + N_{\Lambda_c} m_{\Lambda_c}$ is the total mass of the (hyper)nucleus.

In our approach, we assume axial symmetry of the mean field, and the deformed SHF Schrödinger equation is solved in cylindrical coordinates (r, z) within the axially deformed harmonic-oscillator basis [24–27]. This allows us to make calculations of axially deformed (hyper)nuclei with a quadrupole constraint. The optimal quadrupole deformation parameters,

$$\beta_2^{(q)} \equiv \sqrt{\frac{\pi}{5}} \frac{\langle 2z^2 - r^2 \rangle_q}{\langle r^2 + z^2 \rangle_q}, \tag{13}$$

are determined by minimizing the energy-density functional, while the rms radii are given by

$$R_q \equiv \sqrt{\langle r^2 + z^2 \rangle_q}. \tag{14}$$

Note that in this work, we reduce the SLy4 s.o. interaction strength for ^{12}C and its corresponding Λ and Λ_c hypernuclei to 60%, as in Refs. [50,51], to obtain a reasonable deformation of the ground state of ^{12}C.

The calculated results of these observables will be discussed in the next section, together with the Λ and Λ_c separation energies

$$B_\Lambda \equiv E[^{A-1}(Z)] - E\left[^{A}_{\Lambda}Z\right], \tag{15}$$

$$B_{\Lambda_c} \equiv E[^{A-1}(Z-1)] - E\left[^{A}_{\Lambda_c}Z\right]. \tag{16}$$

We now discuss the choice of the five $\Lambda_c N$ interaction parameters a_i, Eq. (7). Due to absence of quantitative data on Λ_c hypernuclei, it is currently impossible to determine them. We therefore use the well-constrained parameters for the strange Λ hyperon as a guideline, which were determined in Refs. [41,48] by a simultaneous fit to the current global data set of Λ hypernuclei, and the optimal values $a_{0,1,2,3} = [-322.0, 15.75, 19.63, 715.0]$ (in appropriate units for ρ given in fm^{-3} and ε in MeV fm^{-3}) were obtained. In the absence of further information, we then introduce a global scaling factor K for the parameters $a_{0,1,2,3}$, and will study in the following the dependence of the results on this parameter, in particular in comparison with the results of other approaches, as listed in Table I.

The parameter a_4, which governs the $\Lambda_c N$ s.o. splitting, is already very small for Λ hypernuclei [29,52,53], and a strong reduction of spin orbitals in the $\Lambda_c N$ channels was found based on the quark substructure of hadrons [54]. Due to the large mass of the Λ_c baryon, an even smaller s.o. splitting may occur in Λ_c hypernuclei. Therefore, we omit here the $\Lambda_c N$ s.o. interaction.

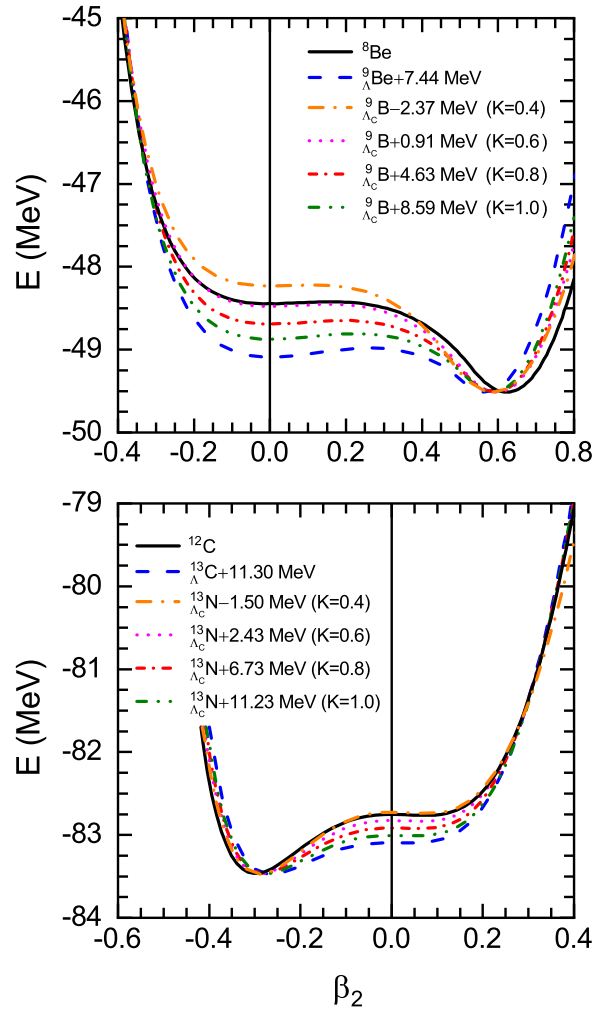

FIG. 1. The calculated potential energy surfaces as functions of the total quadrupole deformation β_2 for ^{8}Be and ^{12}C and their corresponding $1s$ Λ and Λ_c hypernuclei $^{9}_{\Lambda}$Be and $^{9}_{\Lambda_c}$B as well as $^{13}_{\Lambda}$C and $^{13}_{\Lambda_c}$N, obtained with different $\Lambda_c N$ interaction strengths $K = 0.4$, 0.6, 0.8, 1.0. The energies of the hypernuclei are shifted with respect to those of their core nuclei, as specified in the legend.

III. RESULTS

In the following, we compare the properties of Λ and Λ_c hypernuclei and the dependence on the $\Lambda_c N$ interaction parameter K. Compared to the Λ, the Λ_c features two important differences: its much larger mass, and its positive electric charge. The first one leads to a strong reduction (about 1/2) of the Λ_c kinetic energy, in particular in light and small nuclei, whereas the additional Coulomb repulsion becomes dominant in heavier nuclei. The competition between both effects will clearly be seen in the following.

A. Potential energy curves

The impurity effect of an s-state hyperon is often reflected by a deformation reduction of the nuclear core [30,55–60]. In order to study this effect for Λ_c hypernuclei, we show in Fig. 1 the calculated potential energy surfaces (PESs) as functions of the quadrupole deformation parameter β_2 for ^{8}Be, ^{12}C, and

TABLE II. The calculated deformations, radii (in fm), and energies (in MeV), for different $Y = \Lambda, \Lambda_c$ (hyper)nuclei. The last two columns compare B_Y values of DSHF and spherical SHF calculations.

	K	β_2	$\beta_2^{(N)}$	$\beta_2^{(Y)}$	R_N	R_Y	$-E$	$B_Y^{(\mathrm{def.})}$	$B_Y^{(\mathrm{sph.})}$
^{8}Be		0.622	0.621		2.548		49.51		
$^{9}_{\Lambda}$Be		0.566	0.592	0.308	2.484	2.200	56.95	7.44	8.08
$^{9}_{\Lambda_c}$B	1.0	0.586	0.596	0.435	2.494	1.793	58.10	8.59	9.02
$^{9}_{\Lambda_c}$B	0.9	0.589	0.600	0.429	2.504	1.845	56.10	6.59	6.93
$^{9}_{\Lambda_c}$B	0.8	0.594	0.606	0.424	2.516	1.912	54.14	4.63	4.88
$^{9}_{\Lambda_c}$B	0.7	0.595	0.609	0.410	2.526	1.996	52.25	2.74	2.88
$^{9}_{\Lambda_c}$B	0.6	0.597	0.615	0.393	2.539	2.115	50.42	0.91	0.94
$^{9}_{\Lambda_c}$B	0.5	0.594	0.618	0.362	2.549	2.297	48.71	−0.80	−0.90
$^{9}_{\Lambda_c}$B	0.4	0.588	0.624	0.325	2.563	2.651	47.14	−2.37	−2.58
^{12}C		−0.299	−0.298		2.595		83.47		
$^{13}_{\Lambda}$C		−0.262	−0.269	−0.154	2.547	2.168	94.77	11.30	11.64
$^{13}_{\Lambda_c}$N	1.0	−0.277	−0.280	−0.211	2.558	1.850	94.70	11.23	11.49
$^{13}_{\Lambda_c}$N	0.9	−0.280	−0.283	−0.209	2.564	1.896	92.43	8.96	9.18
$^{13}_{\Lambda_c}$N	0.8	−0.282	−0.286	−0.205	2.570	1.952	90.20	6.73	6.91
$^{13}_{\Lambda_c}$N	0.7	−0.284	−0.288	−0.200	2.577	2.025	88.02	4.55	4.68
$^{13}_{\Lambda_c}$N	0.6	−0.286	−0.291	−0.191	2.583	2.124	85.90	2.43	2.51
$^{13}_{\Lambda_c}$N	0.5	−0.290	−0.297	−0.181	2.592	2.276	83.86	0.39	0.42
$^{13}_{\Lambda_c}$N	0.4	−0.293	−0.303	−0.164	2.601	2.536	81.96	−1.51	−1.53

their corresponding Λ and Λ_c hypernuclei $^{9}_{\Lambda}$Be and $^{9}_{\Lambda_c}$B as well as $^{13}_{\Lambda}$C and $^{13}_{\Lambda_c}$N, for different interaction strengths $K = 0.4, 0.6, 0.8, 1.0$. All (hyper)nuclei are strongly deformed, ^{8}Be prolate ($\beta_2 \approx +0.6$) and ^{12}C oblate ($\beta_2 \approx -0.3$). With an unmodified interaction strength $K = 1$, $^{9}_{\Lambda_c}$B is more bound than $^{9}_{\Lambda}$Be, but $^{13}_{\Lambda_c}$N is less bound than $^{13}_{\Lambda}$C. As pointed out above, this is the consequence of the competition between attractive effect of the large Λ_c mass (dominant for very light nuclei) and the Coulomb repulsion dominant for heavy nuclei. With decreasing interaction parameter K, the PESs of the Λ_c hypernuclei correspondingly increase together with their deformation β_2. For $K = 0.4$, both $^{9}_{\Lambda_c}$B and $^{13}_{\Lambda_c}$N are unbound.

In Table II we list in detail the values of binding energies, deformations, and radii obtained for the different configurations. The removal energy of the $^{13}_{\Lambda}$C Λ $1s$ state is $B_\Lambda = 11.30$ MeV, in fair agreement with experimental values (see Ref. [61] for a recent compilation) 11.22 ± 0.08 MeV (emulsion), $11.69 \pm 0.12 \pm 0.04$ MeV (emulsion), $11.98 \pm 0.05 \pm 0.08$ MeV (π^+, K^+), 11.0 ± 0.4 MeV (K^-, π^-), which unfortunately do not agree very well. For $^{9}_{\Lambda}$Be the experimental data are $6.71 \pm 0.04 \pm 0.04$ MeV (emulsion), $6.59 \pm 0.07 \pm 0.08$ MeV (π^+, K^+), $6.30 \pm 0.10 \pm 0.10$ MeV (K^-, π^-), compared to the theoretical 7.44 MeV, which is too large, because the SHF mean field cannot account for the 2α cluster structure of this nucleus [62,63]. This might be alleviated in a beyond-mean-field calculation [64].

There are no experimental data for charmed hypernuclei, but the calculated separation energy B_{Λ_c} of $^{13}_{\Lambda_c}$N for $K = 0.8$ is 6.73 MeV, qualitatively consistent with other theoretical approaches [14–18] employing similar $\Lambda_c N$ interaction strengths. The Table II contains also the values of B_Y for the undeformed calculations, which are generally up to about 1 MeV more bound than including deformation. Therefore deformation reduces the binding of hyperon $1s$ states, due to a reduction of the central density of the core nucleus [57]. This is opposite to the effect on $1p$ states [29,53,65] that will be analyzed in more detail later.

Regarding deformations and radii, one notes that with increasing K, the radius R_{Λ_c} decreases, but the deformation $\beta_2^{(\Lambda_c)}$ increases, as the $1s$ Λ_c is more and more molded into the embedding strongly deformed nuclear core. However, the total deformation β_2 of the hypernuclei diminishes, due to the shrinking effect of the added hyperon on the nuclear core.

To visualize better the results, we present in Fig. 2 the density distributions for nucleons and hyperons in the deformed ground states of $^{13}_{\Lambda}$C and $^{13}_{\Lambda_c}$N obtained with $K = 1$. Due to its large mass, the Λ_c is more localized than the Λ, and therefore the central density of Λ_c is significantly higher than that of Λ inside nearly the same nuclear core.

B. Mean fields

To illustrate better the results, we show in Fig. 3 the hyperon total mean fields V_Y, Eq. (6), of the Λ and Λ_c $1s$ hypernuclei with ^{8}Be, ^{12}C, ^{40}Ca, and ^{208}Pb cores, as a function of the radial coordinate r ($z = 0$). The Coulomb field V_C is shown separately for each case. One observes that for $K = 1$ the Λ_c and Λ strong-interaction mean fields $V_Y - q_Y V_C$ are very similar, as the nuclear core is nearly the same in both cases. For smaller values of K, this Λ_c mean field becomes more shallow and for $K \approx 0.8$ is similar to the theoretical values reported in Table I. The main difference between light

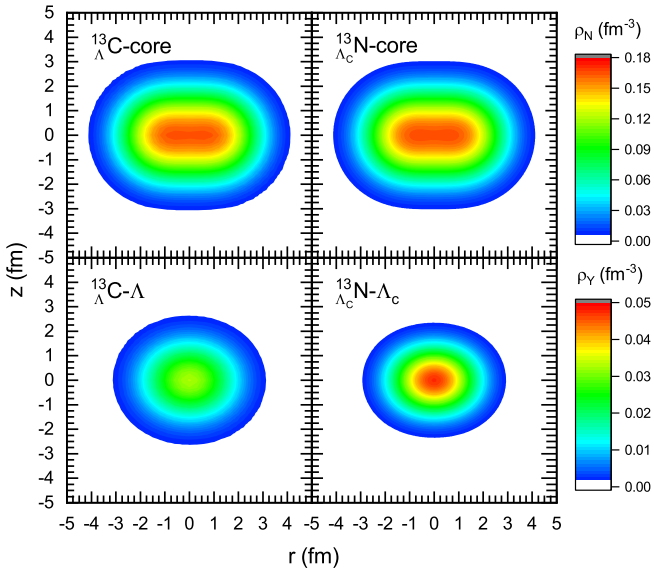

FIG. 2. Contour plots of the nucleon and hyperon densities of $^{13}_{\Lambda}$C and $^{13}_{\Lambda_c}$N ($K = 1$).

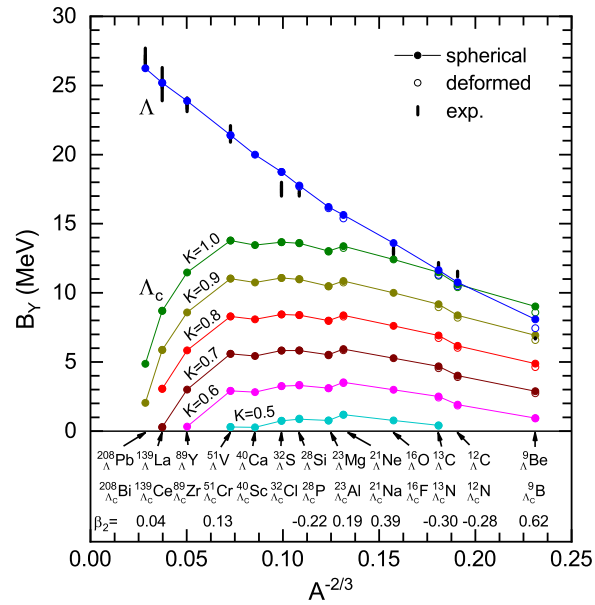

FIG. 4. The hyperon 1s separation energies as a function of mass number A for Λ and Λ_c hypernuclei with different interaction strengths. Results are for spherical calculations (full circles) and deformed ones (open circles), with the deformations β_2 listed in the bottom row. Experimental data for the Λ hypernuclei [67] are also shown.

and heavy nuclei is provided by the Coulomb field, whose magnitude varies from about 4 MeV to 26 MeV going from $^{9}_{\Lambda_c}$B to $^{209}_{\Lambda_c}$Bi, resulting in $V_Y \approx -30$ MeV ($^{13}_{\Lambda}$C) vs -24 MeV ($^{13}_{\Lambda_c}$N, $K = 1$).

The figure shows also the hyperon 1s s.p. levels as horizontal bars. The effect of the Coulomb repulsion for the Λ_c is obvious. It is also notable that the Λ_c states are much deeper bound inside their respective mean field than the Λ, which is a consequence of the larger mass and smaller kinetic energy. In the case of the ^{8}Be core, this leads to a stronger binding of the Λ_c ($K = 1$) than the Λ, in spite of the Coulomb repulsion.

C. Λ_c drip point

These features influence strongly the capability of a nuclear core to bind a Λ_c, which is summarized in Fig. 4, showing the Λ and Λ_c separation energies, Eqs. (15), (16), of various typical nuclei with varying mass number, for different values of the interaction strength $K = 0.5, 0.6, 0.7, 0.8, 0.9, 1.0$. We have chosen to compare hypernuclei with the same nuclear core, for which experimental Λ-hypernuclear data are available, even if the corresponding

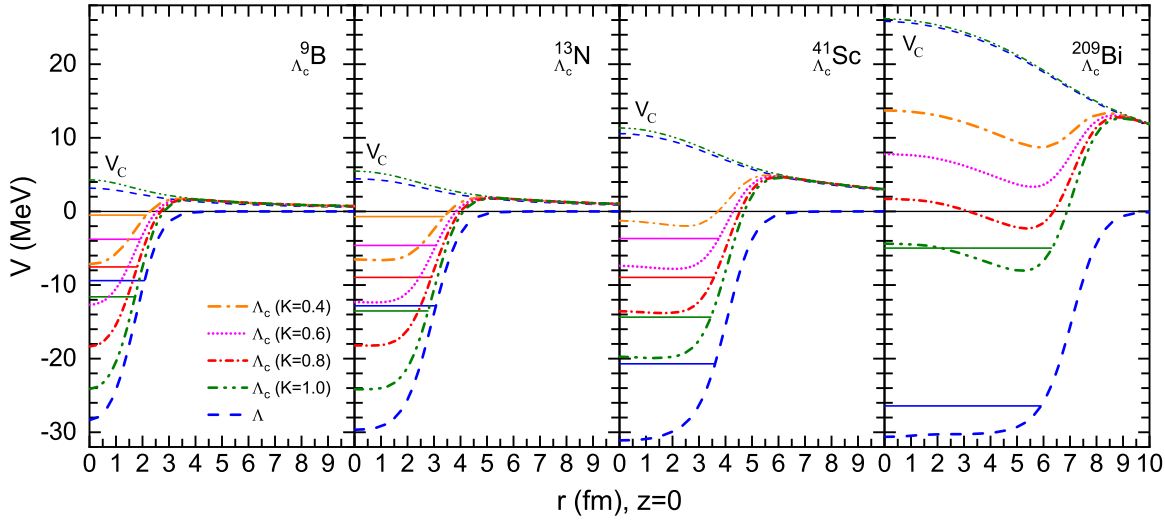

FIG. 3. Λ mean field in $^{9}_{\Lambda}$Be, $^{13}_{\Lambda}$C, $^{41}_{\Lambda}$Ca, $^{209}_{\Lambda}$Pb and Λ_c mean field in $^{9}_{\Lambda_c}$B, $^{13}_{\Lambda_c}$N, $^{41}_{\Lambda_c}$Sc, $^{209}_{\Lambda_c}$Bi as a function of radial coordinate r ($z = 0$). In the latter case different scaling parameters $K = 0.4, 0.6, 0.8, 1.0$ are used. The Coulomb field V_C is also shown (thin curves). Horizontal lines indicate the hyperon 1s s.p. levels.

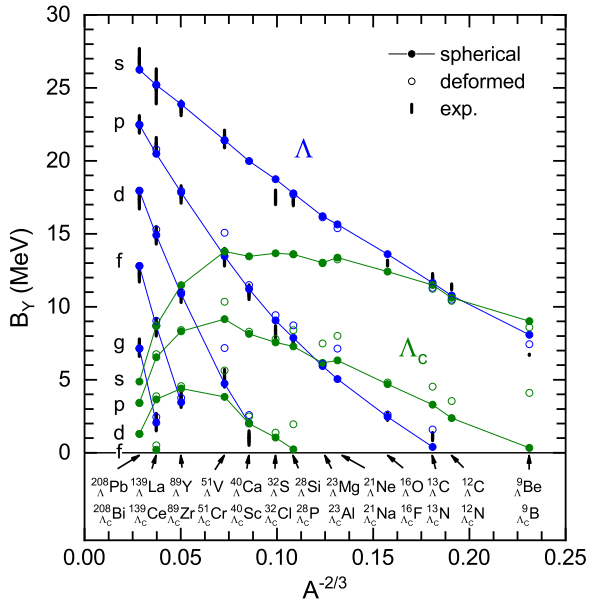

FIG. 5. Same as Fig. 4, but for the hyperon $1s, p, d, f, g$ s.p. states of Λ and $\Lambda_c(K = 1)$ hypernuclei. Only the most bound deformed states are shown.

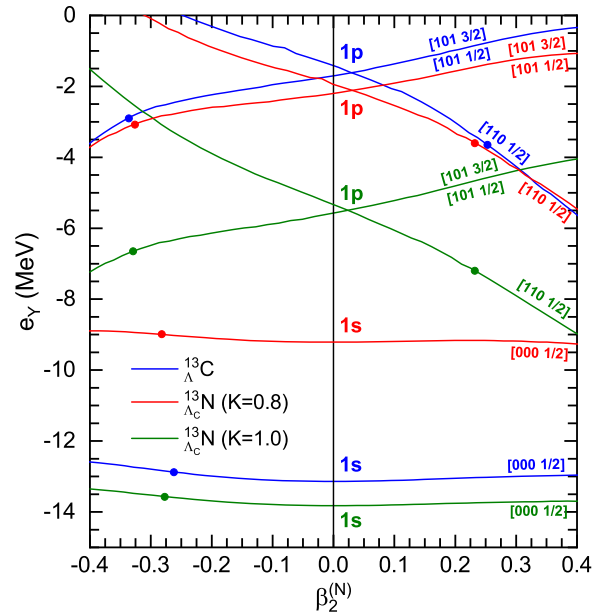

FIG. 6. The hyperon s.p. levels as functions of the core quadrupole deformation $\beta_2^{(N)}$ for ${}^{13}_{\Lambda}$C and ${}^{13}_{\Lambda_c}$N ($K = 0.8, 1.0$). The deformed quantum numbers $[Nn_zm_l\ \Omega]$ label the curves. The physical deformation minima for the various occupied states are indicated by markers.

Λ_c hypernuclei might not be convenient to produce experimentally.

Contrary to Λ hypernuclei, Λ_c hypernuclei reach a maximum binding energy at $A \approx 20, \ldots, 50$ for each interaction strength K, and the upper limit $A_{\max}$ for binding depends on K. The limiting values for the binding of ${}^{209}_{\Lambda_c}$Bi, ${}^{139}_{\Lambda_c}$Ce, ${}^{89}_{\Lambda_c}$Zr, and ${}^{51}_{\Lambda_c}$Cr are $K \gtrsim 0.80, 0.70, 0.60, 0.50$, respectively. Thus even for a rather weak $\Lambda_c N$ interaction $K = 0.5$ some medium-sized Λ_c hypernuclei are still predicted to exist as weakly bound states of about 1 MeV.

The results are qualitatively similar to those of Refs. [12,17,18,66], which also predict Λ_c binding over the full range of A, with a maximum of order 10 MeV. The differences with other works [14–16] can be attributed to the use of very different $\Lambda_c N$ interactions, see Ref. [18]. In particular the lattice QCD results [14] were obtained with an unphysical pion mass $m_\pi = 410$ MeV and grossly underestimate the Λ_c binding in nuclear matter.

The figure comprises various spherical or deformed nuclei, denoted by full or open markers, respectively. The effect of deformation on the $1s$ separation energies (reduction) is fairly small and only visible for the light nuclei and large K, where it might amount to some 100 keV's, see also Table I.

D. *p*-state hypernuclei

The situation is different for higher-l states, which we analyze in Fig. 5 that compares the hyperon $1s, p, d, f, g$ levels of Λ and Λ_c ($K = 1$) hypernuclei, i.e., with the same YN interaction strength. Apart from the qualitatively different behavior due to the Coulomb interaction, Λ_c hypernuclei feature a much smaller level spacing due to the large Λ_c mass, i.e., the p, etc., states are relatively much stronger bound than in Λ hypernuclei. This can clearly be seen in the figure for $A \lesssim 23$, where the $1p$ state is stronger bound in Λ_c than in Λ hypernuclei, in spite of the additional Coulomb repulsion. In fact bound $1p$ states are only obtained for ${}^{12}_{\Lambda_c}$N and ${}^{9}_{\Lambda_c}$B, and $1d$ states only for ${}^{32}_{\Lambda_c}$Cl and ${}^{28}_{\Lambda_c}$P, but not for the corresponding Λ hypernuclei.

Furthermore, in deformed nuclei the $l > 0$ states with the same symmetry as the deformed core are energetically preferred and gain energy compared to the spherical calculation [29,30,53]. This effect can be substantial and is clearly seen in the figure for the strongly deformed V, Si, Mg, Ne, C, Be core nuclei, which gain energies of $\mathcal{O}(1$ MeV) by this effect.

We analyze the mechanism in more detail in Fig. 6, which shows the hyperon $1s$ and $1p$ s.p. levels as functions of $\beta_2^{(N)}$ for ${}^{13}_{\Lambda}$C and ${}^{13}_{\Lambda_c}$N ($K = 0.8, 1$). Markers indicate the physical deformation minima in each case. In the current calculations neglecting the YN s.o. interaction, the [101 1/2] and [101 3/2] $1p$ orbits are degenerate. Their energies are lower than the [110 1/2] orbits on the oblate side (where the physical deformation minima are located at $\beta_2 \approx -0.33$) and higher than the [110 1/2] orbits on the prolate side. The matching deformation characteristics of the embedding core and the [101] orbitals lead to a substantial gain of binding energy of these states, as has been analyzed for Λ hypernuclei in Refs. [29,30,53]. At the physical deformation $\beta_2 \approx -0.33$, the gain of binding energy by deformation of the [101] states is about 2 MeV, as also shown in Fig. 5. In particular at large deformation, this effect amplifies the already stronger bound p states in Λ_c hypernuclei compared to Λ hypernuclei, as shown in Fig. 5, caused by the smaller level spacing for the heavy Λ_c particle. Even for a reduction $K = 0.8$, the Λ_c [101] $1p$ state is still bound with a s.p. energy of about -3 MeV, together

with the [000] $1s$ state at about -9 MeV. For $K \lesssim 0.6$, the Λ_c $1p$ states are not bound anymore, however.

IV. SUMMARY

We investigated Λ_c hypernuclei in the framework of the deformed SHF mean-field model with a combination of the NN interaction SLy4 and a scaled version of the ΛN interaction SLL4 for the $\Lambda_c N$ channel.

Deformation has a small weakening effect on the Λ_c $1s$ states, but might substantially increase the binding of the $1p$ states with the same symmetry as the deformed core. This effect amplifies the small level spacing for the heavy Λ_c particle.

The existence limit of charmed hypernuclei due to the competition between small hyperon kinetic energy and Coulomb repulsion was also studied. With an interaction suppression factor $K \gtrsim 0.8$ charmed hypernuclei exist over the full mass range $A < 208$, whereas for weaker interaction heavy hypernuclei cease to exist gradually. Even for $K = 0.5$, some medium-size Λ_c hypernuclei still exist.

Further quantitative theoretical explorations have to await the availability of reliable experimental data.

ACKNOWLEDGMENTS

This work was supported by the National Natural Science Foundation of China under Grants No. 12175071 and No. 12205103.

[1] C. B. Dover and S. H. Kahana, Phys. Rev. Lett. **39**, 1506 (1977).
[2] Yu. A. Batusov, S. A. Bunyatov, V. V. Lyukov, V. M. Sidorov, A. A. Tyapkin, and V. A. Yarba, JETP Letters **33**, 52 (1981).
[3] B. F. Gibson, C. B. Dover, G. Bhamathi, and D. R. Lehman, Phys. Rev. C **27**, 2085 (1983).
[4] H. Bandō and M. Bando, Phys. Lett. B **109**, 164 (1982).
[5] H. Bandō and S. Nagata, Prog. Theor. Phys. **69**, 557 (1983).
[6] N. Starkov and V. Tsarev, Nucl. Phys. A **450**, 507 (1986).
[7] V. V. Lyukov, Nuov. Cim. A **102**, 583 (1989).
[8] S. Bunyatov, V. Lyukov, N. Starkov, and V. Tsarev, Nuov. Cim. A **104**, 1361 (1991).
[9] R. Shyam and K. Tsushima, Phys. Lett. B **770**, 236 (2017).
[10] R. Gatto and F. Paccanoni, Nuov. Cim. A **46**, 313 (1978).
[11] G. Bhamathi, Phys. Rev. C **24**, 1816(R) (1981).
[12] H. Bandō, Prog. Theor. Phys. Suppl. **81**, 197 (1985).
[13] Y.-H. Tan, X.-H. Zhong, C.-H. Cai, and P.-Z. Ning, Phys. Rev. C **70**, 054306 (2004).
[14] T. Miyamoto *et al.*, Nucl. Phys. A **971**, 113 (2018).
[15] L. Wu, J. Hu, and H. Shen, Phys. Rev. C **101**, 024303 (2020).
[16] I. Vidaña, A. Ramos, and C. E. Jiménez-Tejero, Phys. Rev. C **99**, 045208 (2019).
[17] J. Haidenbauer, A. Nogga, and I. Vidaña, Eur. Phys. J. A **56**, 1 (2020).
[18] H. Güven, K. Bozkurt, E. Khan, and J. Margueron, Phys. Rev. C **104**, 064306 (2021).
[19] A. Hosaka, T. Hyodo, K. Sudoh, Y. Yamaguchi, and S. Yasui, Prog. Part. Nucl. Phys. **96**, 88 (2017).
[20] X.-R. Zhou, H.-J. Schulze, H. Sagawa, C.-X. Wu, and E.-G. Zhao, Phys. Rev. C **76**, 034312 (2007).
[21] F. Ajzenberg-Selove, Nucl. Phys. A **490**, 1 (1988).
[22] J. Cugnon, A. Lejeune, and H.-J. Schulze, Phys. Rev. C **62**, 064308 (2000).
[23] I. Vidaña, A. Polls, A. Ramos, and H.-J. Schulze, Phys. Rev. C **64**, 044301 (2001).
[24] D. Vautherin, Phys. Rev. C **7**, 296 (1973).
[25] M. Bender, P.-H. Heenen, and P.-G. Reinhard, Rev. Mod. Phys. **75**, 121 (2003).
[26] J. Stone and P.-G. Reinhard, Prog. Part. Nucl. Phys. **58**, 587 (2007).
[27] J. Erler, P. Klüpfel, and P.-G. Reinhard, J. Phys. G: Nucl. Part. Phys. **38**, 033101 (2011).
[28] J. Guo, C. F. Chen, X.-R. Zhou, Q. B. Chen, and H.-J. Schulze, Phys. Rev. C **105**, 034322 (2022).
[29] H.-T. Xue, Q. B. Chen, X.-R. Zhou, Y.-Y. Cheng, and H.-J. Schulze, Phys. Rev. C **106**, 044306 (2022).
[30] C. F. Chen, Q. B. Chen, X.-R. Zhou, Y.-Y. Cheng, J.-W. Cui, and H.-J. Schulze, Chin. Phys. C **46**, 064109 (2022).
[31] Y.-F. Chen, X.-R. Zhou, Q. B. Chen, and Y.-Y. Cheng, Eur. Phys. J. A **58**, 21 (2022).
[32] Y. Jin, X.-R. Zhou, Y.-Y. Cheng, and H.-J. Schulze, Eur. Phys. J. A **56**, 135 (2020).
[33] J. Guo, X.-R. Zhou, and H.-J. Schulze, Phys. Rev. C **104**, L061307 (2021).
[34] Y. Jin, C. F. Chen, X.-R. Zhou, Y.-Y. Cheng, and H.-J. Schulze, Prog. Theor. Phys. **2019**, 123D03 (2019).
[35] J. Guo, D. H. Chen, X.-R. Zhou, Q. B. Chen, and H.-J. Schulze, Chin. Phys. C **46**, 064106 (2022).
[36] K. Ohtani, K. J. Araki, and M. Oka, Phys. Rev. C **96**, 055208 (2017).
[37] S. Yasui, Phys. Rev. C **100**, 065201 (2019).
[38] D. Vautherin and D. M. Brink, Phys. Rev. C **5**, 626 (1972).
[39] M. Rayet, Ann. Phys. **102**, 226 (1976).
[40] M. Rayet, Nucl. Phys. A **367**, 381 (1981).
[41] H.-J. Schulze and E. Hiyama, Phys. Rev. C **90**, 047301 (2014).
[42] M. Bender, K. Rutz, P. G. Reinhard, J. A. Maruhn, and W. Greiner, Phys. Rev. C **60**, 034304 (1999).
[43] N. Tajima, P. Bonche, H. Flocard, P.-H. Heenen, and M. Weiss, Nucl. Phys. A **551**, 434 (1993).
[44] T. Suzuki, H. Sagawa, and K. Hagino, Phys. Rev. C **68**, 014317 (2003).
[45] M. Bender, K. Rutz, P.-G. Reinhard, and J. Maruhn, Eur. Phys. J. A **8**, 59 (2000).
[46] P. Ring and P. Schuck, *The Nuclear Many-Body Problem* (Springer Science & Business Media, New York, 1980).
[47] E. Chabanat, P. Bonche, P. Haensel, J. Meyer, and R. Schaeffer, Nucl. Phys. A **635**, 231 (1998).
[48] H.-J. Schulze, AIP Conf. Proc. **2130**, 020009 (2019).
[49] B. Aubert *et al.*, Phys. Rev. D **72**, 052006 (2005).

[50] H. Sagawa, X.-R. Zhou, X. Z. Zhang, and T. Suzuki, Phys. Rev. C **70**, 054316 (2004).
[51] H. Sagawa, X.-R. Zhou, and X. Z. Zhang, Phys. Rev. C **72**, 054311 (2005).
[52] T. Motoba, D. E. Lanskoy, D. J. Millener, and Y. Yamamoto, Nucl. Phys. A **804**, 99 (2008).
[53] H.-T. Xue, Y.-F. Chen, Q. B. Chen, Y. A. Luo, H.-J. Schulze, and X.-R. Zhou, Phys. Rev. C **107**, 044317 (2023).
[54] G. Chanfray and J. Margueron, Phys. Rev. C **102**, 024331 (2020).
[55] E. Hiyama, M. Kamimura, K. Miyazaki, and T. Motoba, Phys. Rev. C **59**, 2351 (1999).
[56] M. T. Win, K. Hagino, and T. Koike, Phys. Rev. C **83**, 014301 (2011).
[57] H.-J. Schulze, M. T. Win, K. Hagino, and H. Sagawa, Prog. Theor. Phys. **123**, 569 (2010).
[58] J. W. Cui, X.-R. Zhou, and H.-J. Schulze, Phys. Rev. C **91**, 054306 (2015).
[59] J. W. Cui, X.-R. Zhou, L. X. Guo, and H.-J. Schulze, Phys. Rev. C **95**, 024323 (2017).
[60] H. Mei, K. Hagino, J. M. Yao, and T. Motoba, Phys. Rev. C **97**, 064318 (2018).
[61] E. Botta, T. Bressani, and A. Feliciello, Nucl. Phys. A **960**, 165 (2017).
[62] H. Bandō, M. Seki, and Y. Shono, Prog. Theor. Phys. **66**, 2118 (1981).
[63] E. Hiyama and T. Yamada, Prog. Part. Nucl. Phys. **63**, 339 (2009).
[64] W.-Y. Li, J.-W. Cui, and X.-R. Zhou, Phys. Rev. C **97**, 034302 (2018).
[65] B.-C. Fang, W.-Y. Li, C.-F. Chen, J.-W. Cui, X.-R. Zhou, and Y.-Y. Cheng, Euro. Phys. J. A **56**, 11 (2020).
[66] K. Tsushima and F. C. Khanna, Phys. Rev. C **67**, 015211 (2003).
[67] A. Gal, E. V. Hungerford, and D. J. Millener, Rev. Mod. Phys. **88**, 035004 (2016).